Martí Albiñana, JV.; Yepes Piqueras, V.; Gonzalez Vidosa, F. (2015). Memetic Algorithm Approach to Designing Precast-Prestressed Concrete Road Bridges with Steel Fiber Reinforcement. Journal of Structural Engineering. 141(2):1-9. doi:10.1061/(ASCE)ST.1943-541X.0001058.

# A memetic algorithm approach to designing of precast-prestressed concrete road bridges with steel fiber-reinforcement

José V. Martí[1], Víctor Yepes [2] and Fernando González-Vidosa, M.ASCE[3]

The formal citation for this paper is:

MARTÍ, J.V.; YEPES, V.; GONZÁLEZ-VIDOSA, F. (2014). **A memetic algorithm approach to designing of precast-prestressed concrete road bridges with steel fiber-reinforcement.** *Journal of Structural Engineering ASCE*, DOI:10.1061/(ASCE)ST.1943-541X.0001058 , 04014114.

Link to published version: http://dx.doi.org/10.1061/(ASCE)ST.1943-541X.0001058



[1] Associate Professor, Institute of Concrete Science and Technology (ICITECH), *Universitat Politècnica de València*, 46022 Valencia, Spain. E-mail: jvmartia@upv.es

[2] Associate Professor, Institute of Concrete Science and Technology (ICITECH), *Universitat Politècnica de València*, 46022 Valencia, Spain. **Corresponding author**. Phone +34963879563; Fax: +34963877569; E-mail: vyepesp@upv.es

[3] Professor, Institute of Concrete Science and Technology (ICITECH), *Universitat Politècnica de València*, 46022 Valencia, Spain. E-mail: fgonzale@upv.es

## Abstract

This paper describes the influence of steel fiber-reinforcement on the design of cost-optimized, prestressed concrete, precast road bridges, with a double U-shaped cross-section and isostatic spans. A memetic algorithm with variable-depth neighborhood search (MA-VDNS) is applied to the economic cost of these structures at different stages of manufacturing, transportation and construction. The problem involved 41 discrete design variables for the geometry of the beam and the slab, materials in the two elements, active and passive reinforcement, as well as residual flexural tensile strength corresponding to the fibers. The use of fibers decreases the mean weight of the beam by 1.72%, reduces the number of strands an average of 3.59%, but it increases the passive reinforcement by 8.71% on average, respectively. Finally, despite the higher cost of the fibers, their use is economically feasible since the average relative difference in cost is less than 0.19%.



**Keywords:** Heuristic optimization; precast beam; prestressed concrete bridge; steel fiber; structural design.

## Introduction

For more than half a century, precast-prestressed concrete (PPC), pretensioned concrete beams with cast-in-situ slabs has been one of the most common forms of structural systems when building road bridges, given their cost effectiveness, especially when high production volumes are possible (Yee 2001). Production control in precast plants not only provides better quality of concrete products (geometry, facing, finishes, etc.), but it also reduces construction time. In this context, standard PPC bridge beams are considered one of the key solutions to bridging problems in the short-to-medium-span range, typically ranging from 10 m to over 40 m.

On the other hand, the stationary precasting industry offers optimal possibilities for steel fiber-reinforced concrete (SFRC) as a cement-based composite material, whose use has increased since steel fibers were introduced as effective concrete reinforcement in the 1960s. Extensive research has shown that dispersed fiber-reinforced in concrete improves such mechanical and fracture properties as tensile strength, energy absorption capacity, toughness, seismic loads resistance, fatigue resistance, cracking resistance and ductility (ACI 1996). These properties are influenced by parameters such as the type of fiber, aspect ratio (length/diameter), fiber content, and distribution as well as their matrix properties. Nowadays, SFRC is increasingly used in structural engineering applications, including pavements and overlays, industrial floors, precast elements, hydraulic and marine structures, large industrial slabs, tunnel linings and in bridge decks. Even though the use of SFRC allows for savings on assembling operations related to conventional reinforcement and for reductions in labor force, equipment use, and associated risks (de la Fuente et al. 2011), steel fibers are often considered expensive. Additionally, reducing material weight through prestressing is essential due to elevation and transportation requirements. This is where structural optimization of this type of large and repetitive structures becomes particularly relevant.

Economic optimization of concrete structures is central in the practice of engineering, not only for savings in materials but also for automating the engineering design process. Most realistic structural optimization problems cannot be addressed by exact methods because computing time becomes prohibitive when large numbers of variables are required. Fortunately, it is now possible to use high-level frameworks which employ heuristics to find acceptable solutions at a reasonable computational cost. Much research has been conducted with the so-called metaheuristics methods in structural engineering (Hare et al. 2013). Design optimization of prestressed concrete (PC) beams is a classical problem considered many years ago (Kirch 1973); however, as Hernandez et al. (2010) have recently suggested, most approaches for beam and slab deck bridges found in the literature are not suitable for implementation in real life engineering. While there is little research on optimization of PC structures (Ohkubo et al. 1998; Sirca and Adeli 2005; Ahsan et al. 2012; Martí et al. 2013), the literature includes numerous studies on optimizing real-life reinforced concrete (Yepes et al. 2012; Paya et al. 2008; Martinez et al. 2010; Carbonell et al. 2011; Camp and Akin 2012; El Semelawy et al. 2012). Sarma and Adeli (1998) reviewed research on cost optimization of concrete structures while Hassanain and Loov (2003) did the same for concrete bridge structures. Regarding SFRC structures, optimization techniques have been employed in recent years in the design of fiber-reinforced concrete mixes (Baykasoglu et al. 2009; Ayan et al. 2011). However, the literature includes very few works on the cost optimization of SRFC structures (Ezeldin and Hsu 1992; Suji et al. 2008). This shows that there is ample research in SRFC cost optimization, especially regarding prestressed fiber-reinforced concrete (PFRC) structures.

In this research, the interest of the authors in the cost optimization of PPC road bridges focuses on the influence of steel-fiber reinforcement (SFR) on the optimal design of this type of structures. The PPC bridge system studied consists of two simply-supported U-beams with a cast-in-situ reinforced concrete slab for road traffic (Fig. 1). A large number of design variables and constraints are considered, and a memetic algorithm with variable-depth neighborhood search is used. In the following sections, the numerical research and parametric study center on the influence of SFR on the optimum cost design of PPC U-beam bridges. After a description of the proposed optimization model, the optimization methodology is presented and verified comparing different lengths of the bridge analyzed as well as the PC and PFRC beams.

## Proposed Optimization Model

The optimization of composite materials such as concrete involves the problem of selecting values for several variables to determine the minimum value for a function subject to design constraints:

$$\min\ C(x) \quad \text{subject to } g_j(x) \le 0, \qquad x_i \in \left(d_{i1}, d_{i2}, \ldots, d_{iq_i}\right) \tag{1}$$

where $C(x)$ denotes the objective function, which represents the cost of building the structure as the sum of unit prices multiplied by the measurements of construction units, and $g_j(x)$ denotes the serviceability limit states (SLSs), the ultimate limit states (ULSs) as well as the geometric constraints of the problem. Each variable $x_i$ can take on the discrete values listed in Eq. (1) because the final solution must be constructable.

The objective function considered, $f_{cost}$, is the cost function defined in the following equation:

$$f_{\cos t} = \sum_{i=1,r} c_i \times u_i\left(x_1, x_2, \ldots, x_n\right) \tag{2}$$

where $c_i$ = unit costs; $u_i$ = amount of material and construction units, and $r$ = total number of construction units. For this study, the basic costs, obtained from a survey of Spanish contractors and subcontractors of precast structures, are given in Tables 1, 2, 3 and 4 (Martí 2010). The cost-related input for placement of fiber reinforcement is included in the cost of the beam steel fiber (Table 1).

The precast bridge is defined using 41 design variables. There are eight geometrical design variables representing the dimensions of the bridge: the depth of the beam ($h_1$), the width of the beam soffit ($b_1$) and the thickness of the bottom flange ($e_1$), the width and thickness of the top flanges of the beam ($b_3$ and $e_3$), the thickness of the webs ($e_2$), the thickness of the slab ($e_4$) and the spacing between beams ($S_v$). Another two variables define the slab and the beam compressive strength of the concrete. The design residual flexural strength of the concrete, $f_{R,3d}$, is a variable necessary to calculate the sections subject to normal stresses in the ULSs. Prestressing is defined by four variables: the number of strands in the top flanges, the number of strands in the the bottom flange, and number of sections with strand sheaths (non-bonded steel) in the second and third layers of the bottom flange. Lastly, 26 variables define the diameters, spacing and lengths of the reinforcing bars following a standard set-up for the beam and the top slab. Table 5 lists parameters established for the structure analyzed, and Fig. 2 shows the main variables and parameters for the beam and slab. The slenderness of the beam is limited to a minimum of $L/17$ due to aesthetic, ground and specific road transportation considerations, where $L$ is the span length. Otherwise, the optimization algorithm tends to increase the depth of the beam continuously, and particulary for short span bridges. The model is flexible since variables and parameters can easily be adapted to the given precast plant process specific needs. The variable traffic load is taken as a uniformly distributed load of 4.0 kN/m$^2$ and a point load of 600 kN, according to IAP-98 code regulation (Ministerio de Fomento 1998). A dead load is assumed as a wearing surface of 0.09 m as well as a uniformly distributed load of 2x0.5 kN/m for concrete bridge barrier rails installed along the edge of the deck. Precast RC slabs of 0.06 m width were considered for the formwork of the top concrete slab. The general exposure class was IIb, according to the Spanish code on structural concrete (EHE-08) (Ministerio de Fomento 2008).

**The Structural Evaluation Module**

Structural constraints considered by the evaluation module followed standard provisions for the Spanish design of this type of structure (Ministerio de Fomento 1998; 2008). Defining a given structure, the structural evaluation module calculates the stress envelopes and checks all the structural constraints. The ULSs for flexure and shear, as well as the geometric minimum requirements, were verified. The calculations for the decompression limit state comprise verifying that under the combination of actions corresponding to the phase being studied, decompression does not occur in the concrete in any fiber in the section. Deflections were limited to 1/1000 of the free span length for the quasi-permanent combination. The ULSs for concrete and steel fatigue were considered in this research. Beam end diaphragms and D-region reinforcement setups can be designed independently in order to resist local stresses and avoid cracking; thus, this was not considered in the optimization process. However, the beam end diaphragms were included for each beam in the structural model. The durability limit state is checked according to the working life design, which was checked at each iteration. The construction sequences and the long-term interaction between the precast beam and the cast-in-place concrete (Marí and Montaler 2000) were considered to design the elements and analyze the structural response of the bridge in each phase. Firstly, a structural model was used for a linear elastic analysis of the beam before being connected to the slab. In this phase, the elastic shortening of concrete was considered when calculating the short-term prestress loss. Then, stress resultants and reactions were calculated taking into account long-term prestress loss due to creeping and shrinkage of concrete and prestressing steel relaxation. A grillage model was used to represent the mechanical characteristics of the bars in which the longitudinal stresses due to the distorsion of the cross-section were considered. The details of the structural model can be found in the work by Martí et al. (2013). To evaluate the sections subject to normal stresses in the ULSs from shear and bending forces, the recommendations indicated in Annex 14 of the EHE-08 (Ministerio de Fomento 2008) were used. Regarding the specified residual characteristic flexural strengths, the following series were used, expressed in $N/mm^2$: 3.0 – 3.5 – 4.0 – 4.5 – 5.0 – 5.5 – 6.0 – 6.5 – 7.0. Common fiber dosages ranging from 40 $kg/m^3$

to 60 kg/m$^3$ can lead to those specified residual characteristic flexural strengths. In spite of the fact that the presence of steel fibers affects the compressive strength and the elasticity modulus (Bentur et al 1990, Nataraja et al 1999, Hatzigeorgiou et al 2005), the stress-strain curve for plain concrete was adopted in this study according to the EHE-08 recommendation (Ministerio de Fomento 2008) as it may be considered that the addition of fibers does not significantly alter the behavior of the concrete under compression. Thus, a rectangular calculation diagram in Fig. 3, characterized by the design residual tensile strength, $f_{ctR,d}$, was used, where $f_{ctR,d} = 0.33 f_{R,3,d}$ and the elongation under maximum load $\varepsilon_{\mathrm{lim}}$ = 20‰ for bending. Skin reinforcement was not required according to the EHE-08 code because of the use of fibers with a structural function (Ministerio de Fomento 2008).

In order to prevent fragile fracture of the concrete, the contribution of the fibers to simple bending was limited following this expression (Ministerio de Fomento 2008):

$$A_p \cdot f_{pd} \frac{d_p}{d_s} + A_s \cdot f_{yd} + \frac{z_f}{z} A_{ct} \cdot f_{ctR,d} \geq \frac{W_1}{z} f_{ctm} + \frac{P}{z}\left(\frac{W_1}{A} + e\right) \tag{3}$$

where $z_f{\cdot}A_{ct}{\cdot}F_{ctR,d}$ is the contribution of the fibers; $z_f$ is the lever arm for the tension in the concrete; $A_{ct}$ is the tensioned area of the concrete, and $f_{ctR,d}$ is the design residual tensile strength in the rectangular diagram. The minimum geometric ratio may be reduced by an equivalent mechanical quantity: $A_c{\cdot}F_{ctR,d}$.

According to the EHE-08 code (Ministerio de Fomento 2008), where there are bent longitudinal bars which are taken into account in the calculation as shear reinforcement, at least one-third of the shear strength must be provided by the contribution of the steel fibers or, where applicable, by the joint contribution of the steel fibers and vertical stirrups. The contribution of the fibers accounted for the load bearing capacity of the tie rods. The failure shear stress due to tension in the web, $V_{u2}$, is equivalent to:

$$V_{u2} = V_{cu} + V_{su} + V_{fu} \tag{4}$$

where $V_{cu}$ is the contribution of the concrete to the shear strength; $V_{su}$ is the contribution of the transverse reinforcement of the web to the shear strength, and $V_{fu}$ is the contribution of the steel fibers to the shear strength. $V_{fu}$ can be evaluated as (Ministerio de Fomento 2008):

$$V_{fu} = 0.7\xi\tau_{fd}b_0d \tag{5}$$

where $\xi = 1 + \sqrt{200/d}$ with $d$ in (mm) and $\xi \leq 2$, and $\tau_{fd}$ is the design value for the increment in shear fiber strength, taking the value $\tau_{fd} = 0.5 \cdot f_{ctR,d}$ (N/mm$^2$).

The minimum quantity of shear reinforcement was provided where the following ratio was met (Ministerio de Fomento 2008):

$$V_{su} + V_{fu} \geq \frac{f_{ct,m}}{7.5}b_0d \tag{6}$$

Regarding longitudinal reinforcements, ($V_{su}$ + $V_{fu}$) was used in the expressions instead of $V_{su}$.

## Proposed Optimization Methodology

A Memetic Algorithm (MA) is a population-based approach to stochastic optimization that combines the parallel search of evolutionary algorithms with the local search of the solutions forming a population (Moscato 1989). The idea of using hybrid population-based and trajectory-based metaheuristics can improve effectiveness by combining diversification and intensification searches (Krasnogor and Smith 2005; Blum et al. 2011).

Regarding the local search strategy used within the memetic algorithm, in this paper we propose a variant of the Very Large-Scale Neighborhood Search (VLSN) algorithm. In particular, following the classification proposed by Ahuja et al. (2002), the variant selected belongs to a class of heuristics known as Variable-Depth Neighborhood Search (VDNS). Although one of the first applications of this strategy can be found for the resolution of vehicle routing problems (Lin and Kernighan 1973), this is the first time that this type of local search is used to optimize structures. VDNS is based on a local search which moves from solution to solution in the space of candidate solutions to reach a local optimum. Then, in order to escape the local optimum, the movement is changed to a larger one, and the search continues until a predefined number of movements, each one larger than the previous. Thus, in this paper, we propose a novel hybrid MA-VDNS to solve structural optimization.

In the MA-VDNS algorithm proposed in this study, the first movement is defined by the random change of a single variable, always choosing the new solution if it improves the previous one. The second movement consists in a simultaneous random change of two variables, and so on. In this case, a number of movements without improvement must be defined to change from one movement to the next. Therefore, the MA-VDNS algorithm begins with the random generation of a population, $N$ = 500 solutions in this case. Each of these solutions is improved by a VDNS local search until a local optimum is reached. To this end, the algorithm begins changing only one variable, and when it takes ten consecutive movements without improvement, the number of variables changing simultaneously is increased to a maximum of eight. Then, a genetic algorithm is applied to this new improved population of 500 solutions. The next step is to create a new generation population of solutions from those selected according to their fitness through crossover and mutation. Appropriate calibration of MA-VDNS algorithm parameters is essential for good MA-VDNS performance. The parameters used in this study are: a population of 500 solutions, probability of 0.50 and elitist selection. A penalty cost is used to evaluate each solution within the evolution procedure; however, the VDNS local search only accepts feasible solutions in order to avoid the early divergence of the algorithm (no penalties are allowed). A VDNS local search is applied to each and every one of the solutions of the new generation. The MA-VDNS will stop if the relative difference between the mean and the minimum cost values at each generation is less than 5%, up to 150 generations. Fig. 4 illustrates typical convergence of the mean and minimum cost curves with the number of generations. Note that the code of the MA-VDNS algorithm can be found in the web page of our research group (www.upv.es/gprc).

## Numerical Results and Parametric Study

The MA-VDNS is used to perform a parametric study with different span lengths to analyze the influence of SFR on cost-optimized precast road bridges. The algorithm was coded in Intel® Visual Fortran Compiler Integration for Microsoft Visual Studio 2008. A typical MA-VDNS run lasted 1300 min for an INTEL® Core TM i7 CPU X980 3.33 GHz. Five span lengths of 20, 25, 30, 35 and 40 m were considered for each of the two bridge beams, considering the parameters defined in Table 5. The results of the parametric study indicated the design rules for the PPC road bridges, with a double U-shaped cross-section and isostatic spans, including the use of steel fibers. The algorithm was run nine times for each span length according to the methodology proposed by Payá-Zaforteza et al. (2010) based on the extreme value theory. The difference checked between the minimum cost obtained with the nine MA-VDNS runs and the extreme value estimated using the three-parameter Weibull distribution that fits 300 MA-VDNS results is less than 3.4%. The average deviations of the mean with respect to the minimum for different span lengths are 5.8% and 6.1% for PC and PFRC structures, respectively (Table 6).

The primary economic, geometric and steel reinforcement characteristics were analysed. Tables 7 and 8 summarize the features of the best solutions: Table 7 shows the solutions for the geometry, concrete grade and amount of prestressing steel of the solutions, while Table 8 lists the concrete and reinforcing steel measurements. The influence of steel fibers is discussed together with those of a regression analysis. The functional relations between the variables are valid approximations within the range of the observational data and therefore require careful consideration when extrapolation is carried out. Fig. 5 shows that there is hardly any difference between the average costs of the PC and the PFRC precast road bridges for span lengths ranging from 20-40 m in steps of 5 m. Thus, the relative difference in terms of average cost between the PFRC and the PC bridges with regard to the PC ones is no more than 1.54% (this is the case for a 35 m span, with an average total cost of US$132,135 and US$134,199 for PFRC and PC bridges, respectively). The average minimum cost per unit area is US$298.62/$m^2$ and US$297.43/$m^2$ for the optimized PC and PFRC bridges, respectively, for span lengths ranging from 20-40 m. In addition, the relative difference in terms of the overall cost per unit area between the 20 and 40 meter spans for the optimized PFRC bridges is no more than 3.80%; in case of optimized PC ones, this relative difference is no more than 4.67%. In this study, decompression does not occur in the concrete in any fiber in the section; thus, the examined beams are under compression due to prestress, while the most benefits of usage of steel fibers have mainly to do with the improvement of concrete behavior in tension or flexure. The cost variation as a function of the horizontal span leads to a high linear correlation. The average PFRC bridge cost adjusts to $C$ = 4123.7 $L$ -9753.2 with a regression coefficient of $R^2$=0.9928, whereas the PC bridge adjusts to $C$ = 3915 $L$ -3609.9 with $R^2$=0.9967. The cost increases as the span lengthens given the higher material costs, necessary to resist increased slab forces and to satisfy deflection requirements. The use of fibers has little effect on the average costs of the precast road bridges despite the fact that PFRC is significantly more expensive than plain concrete (e.g., according to Table 1, the beam concrete HP-45 costs US$197.73/$m^3$; however, the fiber addition of 60 kg/$m^3$ increases the initial cost by nearly 43.4%.) This is a significant finding because the cost of using fibers is clearly advantageous without any loss of competitiveness. Fig. 6 shows the relationship between the mean depth of the beam ($h_1$) and the span lengths for PC and PFRC precast bridges. Again, the use of fibers has no significant influence on the depth of the beam. This is explained by the fact that the ratio $L/h_1$, although limited to $L$/17 (see Table 5), was always lower than $L$/18. The mean depth of the PFRC beam is 2.41% less than the PC one. In the case of a 20 m span, the mean depth of the PFRC beam is less than 0.05 m. The average depth of the beam adjusts to $h_1$ = 0.0488 $L$ + 0.1429 with $R^2$ = 0.9994 in the case of PC bridges and to $h_1$ = 0.0507 $L$ + 0.0524 with $R^2$ = 0.9999 when fibers are used.

In both cases, the value of $R^2$ is near 1.0 which means that the line fits the data almost perfectly. The use of SFR in the beam leads to an average 0.86% reduction in the slab thickness ($e_4$). Regarding the average number of strands in relation to the span, Fig. 7 illustrates a clear difference when the span is lengthened from 35 m to 40 m using the SFR. The number of strands is reduced by 3.59% on average, which means that steel fiber tensile strength can reduce some of the prestressing action. Regardless of the span length considered, an average reduction of 4.10 strands is achieved when fibers are used, which is equivalent to 775.06 kg. The average number of strands in the PC bridges adjusts to $\#strands = 1.2444\ L + 11.178$ with $R^2 = 0.9564$, whereas for those with PFRC the adjustment is $\#strands = 1.0933\ L + 13.8222$ with $R^2 = 0.959$. In both cases, the relationship is quite strong. There is a slight average reduction (0.86%) in the mean characteristic compressive strength of concrete in the beam ($f_{c,beam}$) as a function of the span when using fibers. There is no significant difference in $f_{c,beam}$ when using PFRC in the beam, with a range between 35 MPa and 40 MPa. The concrete grade used is relatively high although the highest concrete grade considered in the optimization problem was 50 MPa. In regards to the slab, the values of the concrete grade are quite similar to the beam, except for the 35 m span length. There is no clear difference in the width of the beam soffit ($b_1$) when using fibers in the beam; thus, the relative difference between the optimized PFRC and the PC bridges is no greater than 0.52%. The mean width of the PC beam soffit adjusts weakly to $b_1 = 0.0081\ L + 1.1647$ with $R^2 = 0.42$, whereas $b_1 = 0.0031\ L + 1.3173$ with $R^2 = 0.216$ for PFRC beams. In Fig. 9, the tendency is to increase the thickness of the bottom flange ($e_1$) in accordance with the span length; notwithstanding, using PFRC in the beam entails an average reduction of 3.25% in $e_1$. Although there is an increasing trend for $e_1$ when the span length is greater than 25 m and 35 m in the case of PC and PFRC beams, respectively. The mean thickness of the bottom flange adjusts to $e_1 = 0.0023\ L + 0.1076$ with $R^2 = 0.6417$, whereas with PFRC, it is $e_1 = 0.0017\ L + 0.1198$ with $R^2 = 0.7492$.

Regarding the ratio of the volume of concrete ($v_c$) and the surface of the slab ($s_s$), Fig. 10 illustrates the amount of concrete tends to increase with the span length. In fact, the mean volume-to-surface ratio for PC beams has a strong adjustment to $v_c/s_s = 0.002\ L + 0.2251$ with $R^2 = 0.9367$; this means that approximately ninty-three percent of the variation can be explained by the span length. Using fibers, the volume of concrete related to the surface of the slab is lower than that for PC beams when the span length is longer than 25 m. This ratio for PFRC beams has a better fit to a line trend: $v_c/s_s = 0.0015\ L + 0.2358$ with $R^2 = 0.8936$. There is a very slight reduction in the amount of concrete with the span length using fibers in the beam, as well as an average reduction of 1.27% in the volume of concrete per unit surface area of slab. In the case of PC beams, the average amount of concrete required is 0.286 $m^3/m^2$, whereas this value ratio is 0.282 $m^3/m^2$ for PFRC beams, which means a relative reduction of 1.5%.

By analyzing the ratio between the passive reinforcement ($p_r$) of the bridge and the surface of the slab ($s_s$), using PFRC in the beam entails a significant increase (average 27.6%) in $p_r/s_s$ when the span length is 40 m. While it seems logical that the passive reinforcement increases as the span lengthens to resist increased slab forces and to satisfy deflection requirements, surprisingly, the amount of passive reinforcement required is higher when steel fibers are used. This is hard to explain since the fibers contribute to increasing the bending and shear strengths of the beam. However, MA-VDNS leads to a 1.72% reduction in the concrete volume (Table 8) due to the high cost of PFRC which implies passive reinforcement increase. It is worth noting that MA-VDNS can find near-optimal solutions that have similar costs, but are quite different in other respects. Table 7 shows that the characteristic compressive strength of the slab concrete ($f_{c,slab}$) of PC for 40 m case is larger than that of PC what is offset by the slab reinforcement (Table 8). On the other hand, the concrete cross-section should not be reduced too much because fibers reduce the number of strands (Fig. 7), this leading to increase the cross-sectional moment of inertia by reducing the thickness of the beam bottom flange. To sum up, increasing the passive reinforcement and reducing concrete volume and the number of strands minimize PFRC cost. The results in Table 7 show no relationship between these variables and the span length of the beam. The thickness of the webs ($e_2$) was 0.10 m in almost all cases and included fibers. Using SFR in the beam leads to a 16.38% reduction in the average width of the beam top flanges ($b_3$) as well as a 21.79% reduction in the average thickness of the beam top flanges ($e_3$). A particularly relevant aspect related to the transport and placement of the precast concrete structures is the weight of the beam ($w_b$), which varies as a function of the horizontal span and leads to a high linear correlation, as shown in Fig. 11. Although using steel fibers in the beam slightly reduces (1.72%) the mean weight of the beam, the mean weight savings is 2,567.22 kg when the span length is 40 m, and thus a significant 3.27% reduction is found. The mean weight of the PC beam adjusts to $w_b = 2616.4\ L - 29617$ with $R^2 = 0.9801$, while when fibers are used, this weight adjusts to $w_b = 2541.3\ L - 28235$ with $R^2 = 0.9907$. However, there is a considerable difference when comparing the weights of the optimized beams; in fact, cost-optimized PFRC beams weigh 6.7%, 6.2% and 5.7% less than the PC ones when the span lengths are 20 m, 25 m and 40 m, respectively.

## Concluding Remarks

In this paper we study the influence of steel fibers on cost-optimized PPC road bridges, typically formed by two isostatic beams, with a double U-shaped cross-section. A memetic algorithm with variable-depth neighborhood search, abbreviated as MA-VDNS, is used in this study. This algorithm combines the synergy effects of the MA and VDNS. The algorithm eliminates the conventional design process of trial and error, in which engineers follow iterative procedures to design PPC bridges. The analysis reveals that despite the higher cost of the fibers, and considering that decompression does not occur in the concrete in any fiber in the section, the relative difference between the optimized PFRC and the PC bridges is less than 5.36% in the worst case studied, which means that using SFR is economically feasible. The parametric study shows a good correlation between the cost, depth of the beam, weight of the beam and number of strands for PRFC and PC bridges and the beam span length, which can be useful for practicing engineers. The use of fibers in the beam leads to an average reduction of 0.86% and 2.41% in the thickness of the slab and in the depth of the beam, respectively. On average, the number of strands is reduced by 3.59%, which means that steel fiber tensile strength can release some of the prestressing action. Using PFRC in the beams leads to an average 0.86% reduction in the compressive strength of the concrete used in the beam and a 2.53% increase in the compressive strength of the concrete used in the slab. There is a very slight reduction in the amount of concrete with the span length using fibers in the beam, as well as an average reduction of 1.27% in the volume of concrete per unit surface area; however, this reduction is above 6% for the cost-optimized solutions. Surprisingly, using PFRC in the beam results in an average 8.71% increase in the passive reinforcement required per unit surface area of slab despite the fibers increasing the beam strength. This can be explained by the lower concrete volume due to the the high cost of PFRC. Finally, in the cost-optimized beams, using PFRC reduces the mean weight of the beam slightly (1.72%); however, this reduction is above 6% for the cost-optimized solutions. This value might be relevant for the transport and placement of these precast beams. To conclude, the methodology described herein is quite flexible and may be further modificed for use with a continuous U-beam bridge systems or other types of bridge systems considering both superstructure and substructure as well as for high strength concrete with steel fiber beams.

**Acknowledgement**

This work was funded by the Spanish Ministry of Science and Innovation (Research Project BIA2011-23602) and the Universitat Politècnica de València (Research Project PAID-06-12). The authors are grateful to the anonymous reviewers for their constructive comments and useful suggestions. The authors are also grateful to Dr. Debra Westall for her thorough revision

of the manuscript.

## Notations

*The following symbols are used in this paper:*

$a_{bar}$ = Concrete bridge barrier width

$A_{ct}$ = Tensioned area of the concrete

$As6$ = Top longitudinal passive reinforcement of the slab

$As7$ = Bottom longitudinal passive reinforcement of the slab

$b_1$ = Width of the beam soffit

$b_3$ = Width of the top flange of the beam

$C$ = Total cost of bridge

$c_i$ = Unit costs

$d$ = Beam effective depth

$e_1$ = Thickness of bottom flange of the beam

$e_2$ = Thickness of the webs

$e_3$ = Thickness of top flange of the beam

$e_4$ = Thickness of slab

$E_{nt}$ = Bearing center to beam face distance

$f_{c,beam}$ = Characteristic compressive strength of concrete in the beam

$f_{c,slab}$ = Characteristic compressive strength of concrete in the slab

$f_{ctR,d}$ = Design residual tensile strength

$f_{pk}$ = Active prestressing steel (Y1860-S7)

$f_{R,3d}$ = Design residual flexural strength of the concrete

$f_{yk}$ = Passive reinforcing steel (B-500-S)

$g_j$ = Structural constraints

$h_1$ = Depth of beam

$i_4$ = Bottom flange division

$I_a$ = Web inclination

$L$ = Span length

$n$ = Number of design variables

$N$ = Number of solutions in a population

$N_{ai}$ = Top active reinforcement of the beam

$N_{as}$ = Bottom active reinforcement of the beam

$n_{i3}$ = Inclination, bottom flange tablet

$n_{s3}$ = Inclination, top flange tablet

$Q_m$ = Concrete bridge barrier loads

$r$ = Number of construction units

$s_3$ = Top flange division

$S_v$ = Spacing between beams

$t_1$ = Transverse reinforcement of the bottom flange of the beam

$t_2$ = Transverse reinforcement of the web of the beam

$t_3$ = Transverse reinforcement of the top flange of the beam

$t_4$ = Top transverse reinforcement of the slab

$t_5$ = Bottom transverse reinforcement of the slab

$T_d$ = Transport distance (one way)

$t_{ws}$ = Thickness of wearing surface

$u_i$ = Amount of material and construction units

$V_{cu}$ = Contribution of concrete to shear strength

$V_{fu}$ = Contribution of steel fibers to shear strength

$V_{su}$ = Contribution of transverse reinforcement of the web to shear strength

$V_{u2}$ = Failure shear stress from tension in the web

$W$ = PC precast bridge width

$x_1,..,x_n$ = Design variables

$z_f$ = Lever arm for tension in the concrete

$\varepsilon_{\mathrm{lim}}$ = Elongation under maximum load

$\tau_{fd}$ = Design value for the increment in shear strength from the fibers

$\Phi_r$ = Beam surface reinforcement

$\Phi_s$ = Strand diameter

## References

Ahuja, R.K., Ergun, Ö., Orlin, J.B., and Punnen, A.P. (2002). "A survey of very large-scale neighborhood search techniques." *Discrete Applied Mathematics*, 123, 75-102.

Ahsan, R., Rana, S., and Nurul Ghani, S. (2012). "Cost optimum design of posttensioned I-girder bridge using global optimization algorithm." *J. Struct. Eng.*, 138(2), 273-284.

American Concrete Institute. (1996). *State of the art report on fiber reinforced concrete (ACI Comittee 544.1R-96),* Detroit, MT.

Ayan, E., Saatçioglu, Ö., and Turanli, L. (2011). "Parameter optimization on compressive strength of steel fiber reinforced high strength concrete." *Constr. Build. Mater.*, 25(6), 2837-2844.

Baykasoglu, A., Oztas, A., and Ozbay, E. (2009). "Prediction and multi-objective optimization of high-strength concrete parameters via soft computing approaches." *Expert Syst. Appl.*, 36(3), 6145-6155.

Bentur, A., and Mindess, S. (1990). Fiber reinforced cementitious composites. Elsevier Applied Science Elsevier Science Publishers Ltd, London, UK.

Blum, C., Puchinger, J., Raidl, G.R., Roli, A. (2011). “Hybrid metaheuristics in combinatorial optimization: A survey.” *Applied Soft Computing*, 11, 4135-4151.

Camp, C.V., and Akin, A. (2012). “Design of retaining walls using Big Bang-Big Crunch optimization.” *J. Struct. Eng.*, 138(3), 438-448.

Carbonell, A., Gonzalez-Vidosa, F., and Yepes, V. (2011). “Design of reinforced concrete road vaults by heuristic optimization.” *Adv. Eng. Software*, 42(4), 151-159.

de la Fuente, A., Domingues de Figueiredo, A., Aguado, A., Molins, C., and Chama Neto, P.J. (2011). “Experimentation and numerical simulation of steel fiber reinforced concrete pipes.” *Mater. Constr.*, 61(302), 275-288.

El Semelawy, M., Nassef, A.O., and El Damatty, A.A. (2012). “Design of prestressed concrete flat slab using modern heuristic optimization techniques.” *Expert Syst. Appl.*, 39(5), 5758-5766.

Ezeldin, A., and Hsu, C. (1992). “Optimization of reinforced fibrous concrete beams.” *ACI Struct. J.*, 89(1), 106-114.

Hare, W., Nutini, J., and Tesfamariam, S. (2013). “A survey of non-gradient optimization methods in structural engineering.” *Adv. Eng. Software*, 59, 19-28.

Hassanain, M.A., and Loov, R.E. (2003). “Cost optimization of concrete bridge infrastructure.” *Can. J. Civil Eng.*, 30(5), 841-849.

Hatzigeorgiou, G.D., and Beskos, D.E. (2005). “Minimum cost design of fibre-reinforced concrete-filled steel tubular columns.” *J. Constructional Steel Research*, 61(2), 167-182.

Hernández, S., Fontan, A.N., Díaz, J., and Marcos, D. (2010). “VTOP. An improved software for design optimization of prestressed concrete beams.” *Adv. Eng. Software*, 41(3), 415-421.

Kirch, U. (1973). “Optimized prestressing by linear programming.” *Int. J. Numer. Methods Eng.*, 7(2), 125-136.

Krasnogor, N., and Smith, J. (2005). “A tutorial for competent memetic algorithms: model, taxonomy, and design issues.” *IEEE Transactions on Evolutionary Computation*, 9, 474-488.

Lin, S., Kernighan, B. (1973). “An effective heuristic algorithm for the traveling salesman problem.” *Operations Research*, 21, 498-516.

Marí, A.R., and Montaler, J. (2000). “Continuous precast concrete girder and slab bridge decks.” *Proc. ICE-Struct. Build.*, 140(3), 195-206.

Martí, J.V. (2010). *Optimal design bridges boards of prestressed concrete precast beams*. Doctoral thesis, Universitat Politècnica de València, Construction Engineering Dept. (in Spanish).

Martí, J.V., González-Vidosa. F., Yepes, V., and Alcalá, J. (2013). “Design of prestressed concrete precast road bridges with hybrid simulated annealing.” *Eng. Struct.*, 48, 342-352.

Martinez, F. J., Gonzalez-Vidosa, F., Hospitaler, A., and Yepes, V. (2010). “Heuristic Optimization of RC Bridge Piers with Rectangular Hollow Sections.” *Comput. Struct.*, 88(5-6), 375-386.

Ministerio de Fomento. (1998). *IAP-98: Code on the actions for the design of road bridges*. IAP-98, Ministerio de Fomento, Madrid, Spain (in Spanish).

Ministerio de Fomento. (2008). *Code of structural concrete*. EHE-08, Ministerio de Fomento, Madrid, Spain (in Spanish).

Moscato, P. (1989). On evolution, search, optimization, genetic algorithms and martial arts: Towards memetic algorithms, Technical Report Caltech Concurrent Computation Program Report 826, Caltech, Pasadena, California, USA.

Nataraja, M.C., Dhang, N., and Gupta, A.P. (1999). “Stress-strain curves for steel-fiber reinforced concrete under compression.” *Cement & Concrete Composites*, 21(5-6), 383-390.

Ohkubo, S., Dissanayake, P.B.R., and Taniwaki, K. (1998). “An approach to multicriteria fuzzy optimization of a prestressed concrete bridge system considering cost and aesthetic feeling.” *Struct. Optim.* 15(2), 132-140.

Payá, I., Yepes, V., González-Vidosa, F., and Hospitaler, A. (2008). “Multiobjective Optimization of Reinforced Concrete Building Frames by Simulated Annealing.” *Comput.-Aided Civ. Infrastruct. Eng.*, 23(8), 596-610.

Payá-Zaforteza, I., Yepes, V., González-Vidosa, F., and Hospitaler, A. (2010). “On the Weibull cost estimation of building frames designed by simulated annealing.” *Meccanica*, 45(5), 693-704.

Sarma, K. C., and Adeli, H. (1998). “Cost optimization of concrete structures.” *J. Struct. Eng.*, 124(5), 570-579.

Sirca, G. F., and Adeli, H. (2005). “Cost optimization of prestressed concrete bridges.” *J. Struct. Eng.*, 131(3), 380-388.

Suji, D., Natesan, S.C., Murugesan, R., and Sanjai Prabhu, R. (2008). “Optimal design of fibrous concrete beams through simulated annealing.” *Asian J. Civ. Eng.*, 9(2), 193-213.

Yee, A.A. (2001). “Social and environmental benefits of precast concrete technology.” *PCI J.*, 46, 14-20.

Yepes, V., González-Vidosa, F., Alcalá, J., and Villalba, P. (2012). “$CO_2$-Optimization design of reinforced concrete retaining walls based on a VNS-threshold acceptance strategy.” *J. Comput. Civ. Eng.*, 26(3), 378-386.

**List of Figures and Tables**

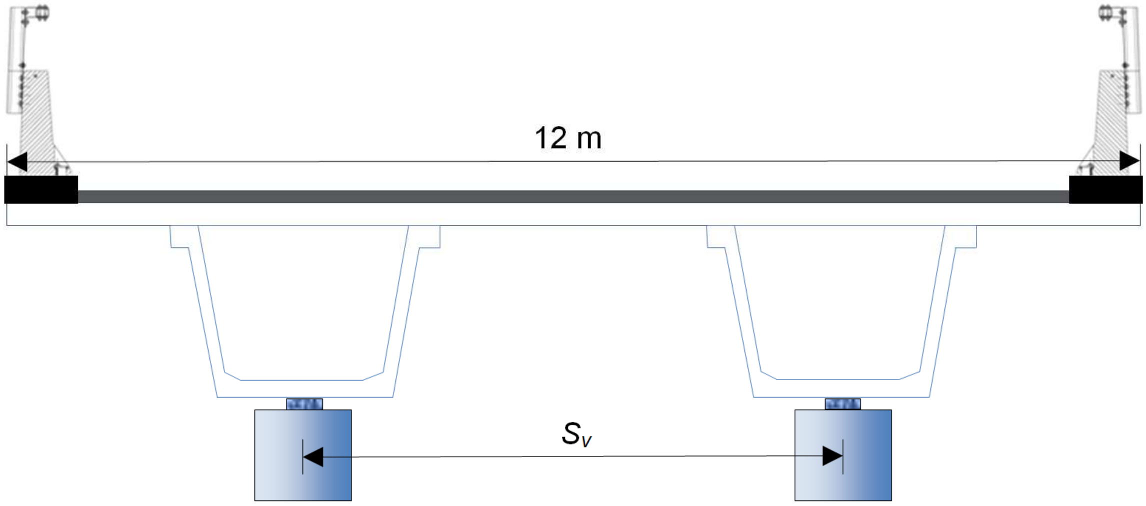


**Fig. 1.** PPC road bridge cross-section

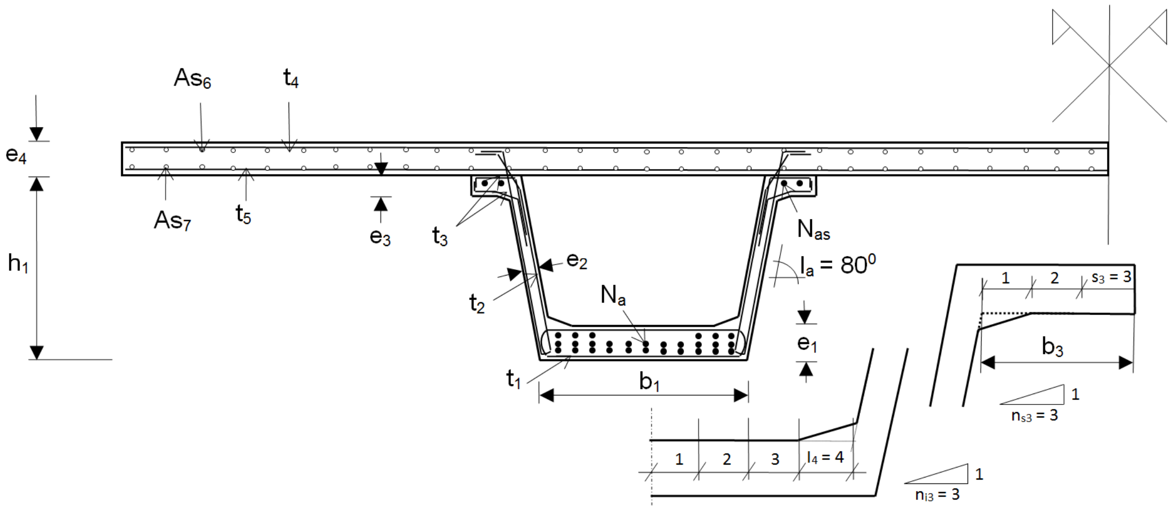


**Fig. 2.** Beam-slab geometric variables, active and passive reinforcement variables, and parameters

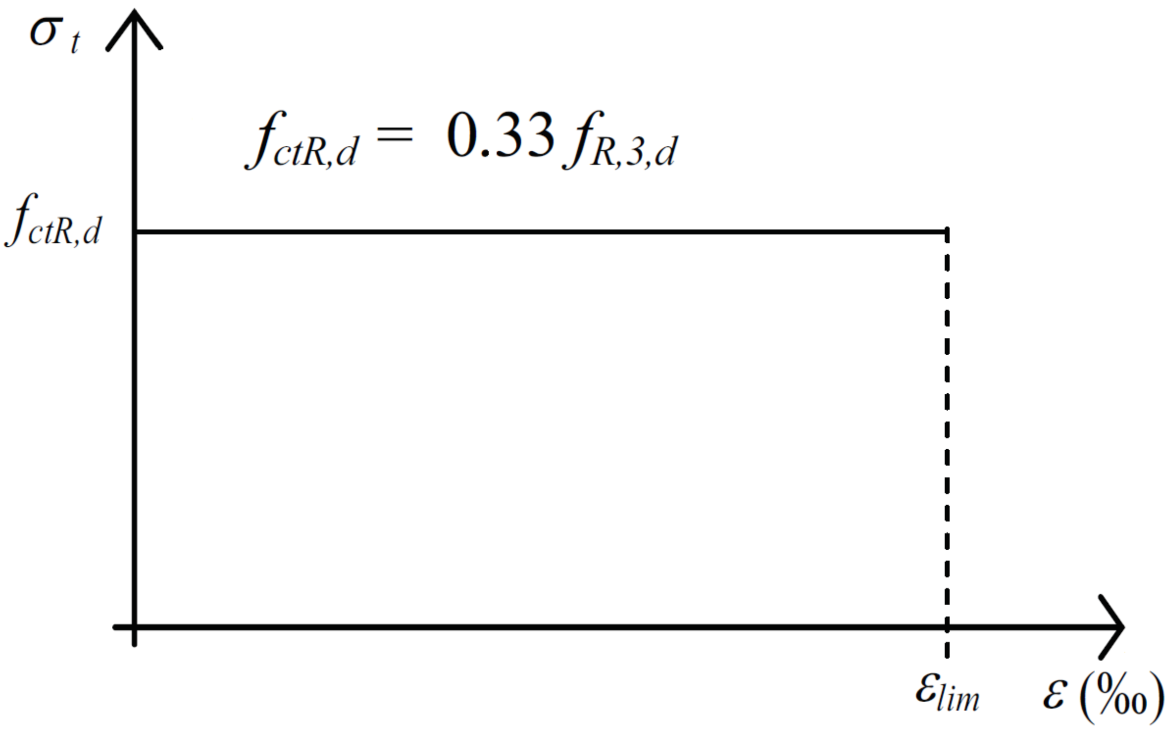


**Fig. 3.** Rectangular calculation diagram of concrete with fibers

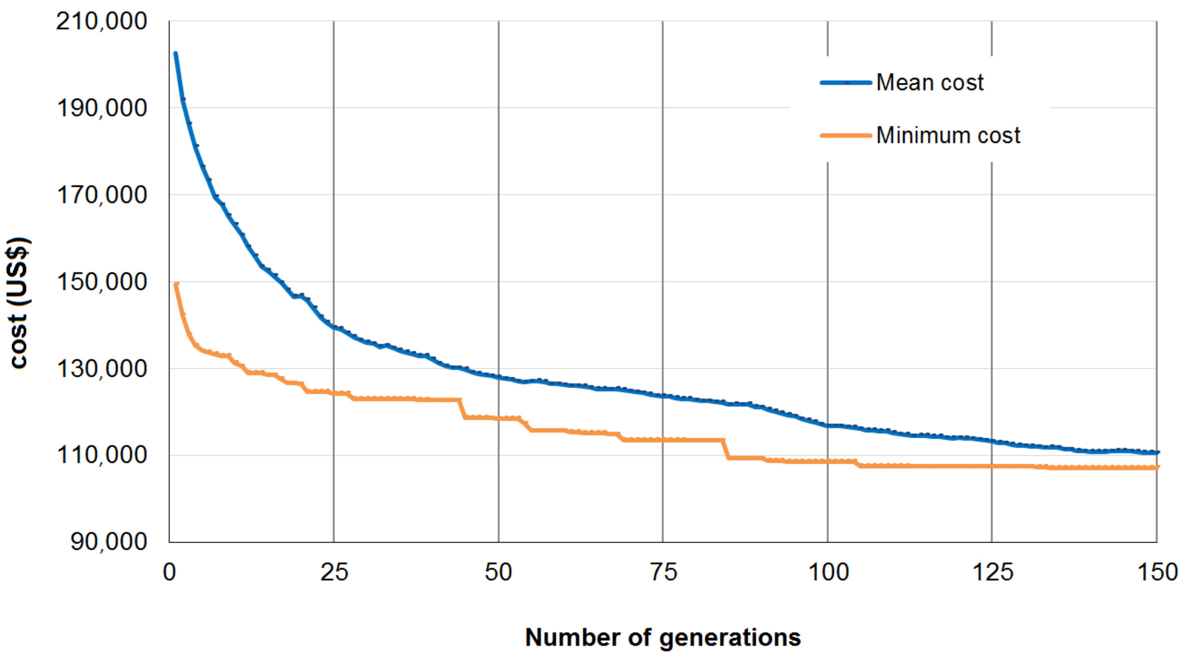


**Fig. 4**. Typical MA-VDNS convergence of the mean and minimum cost curves with the number of generations for PFRC for 30 m span

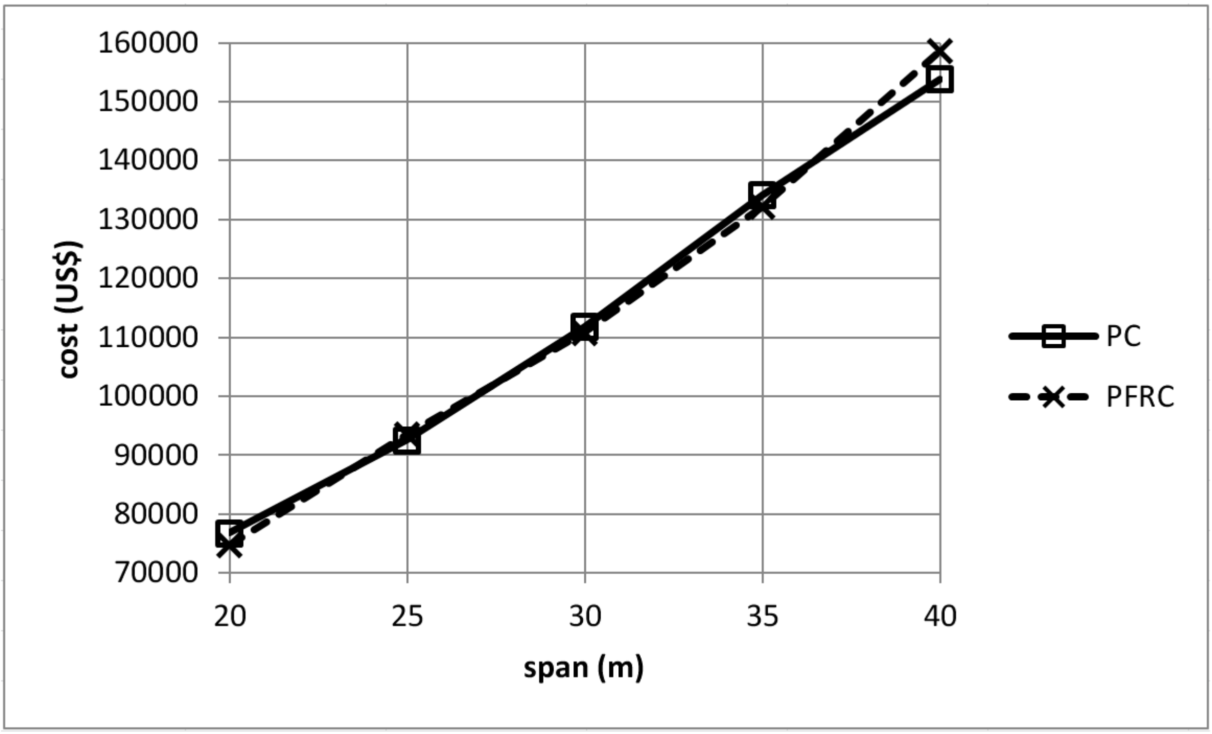


**Fig. 5.** PC and PFRC precast road bridges mean costs for different span lengths

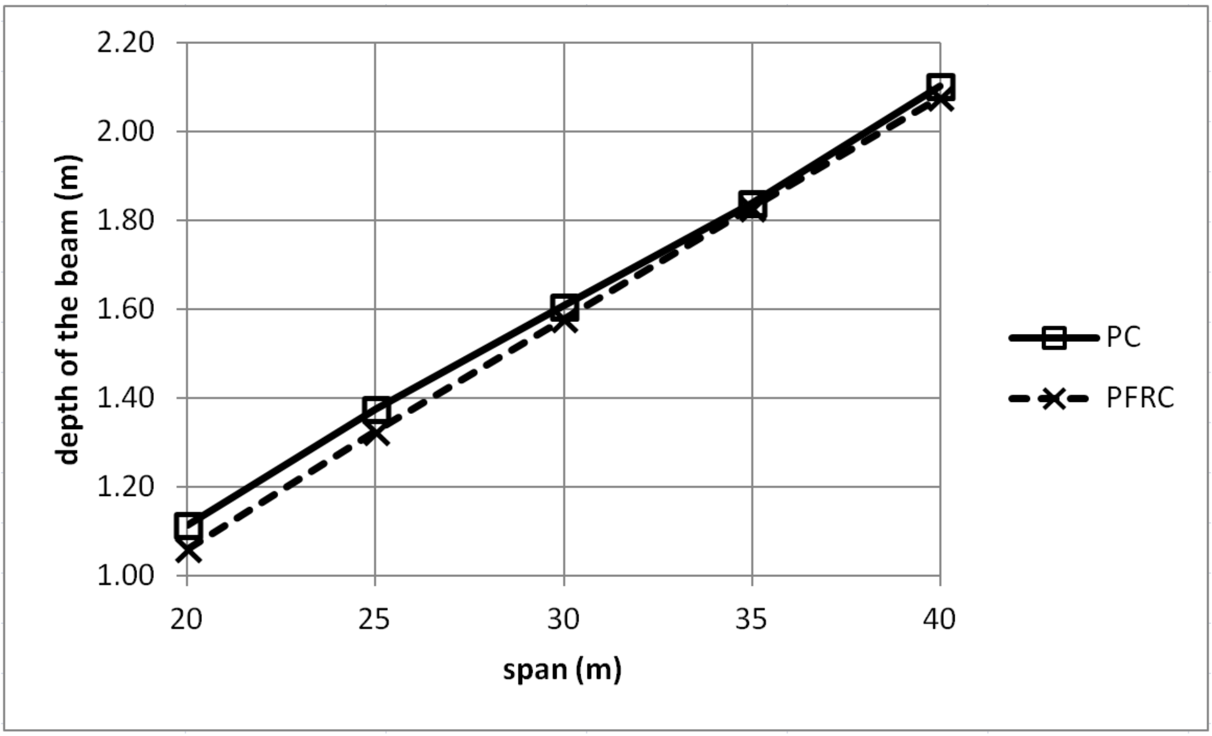


**Fig. 6.** Mean depth of the PC and PFRC beams for different span lengths

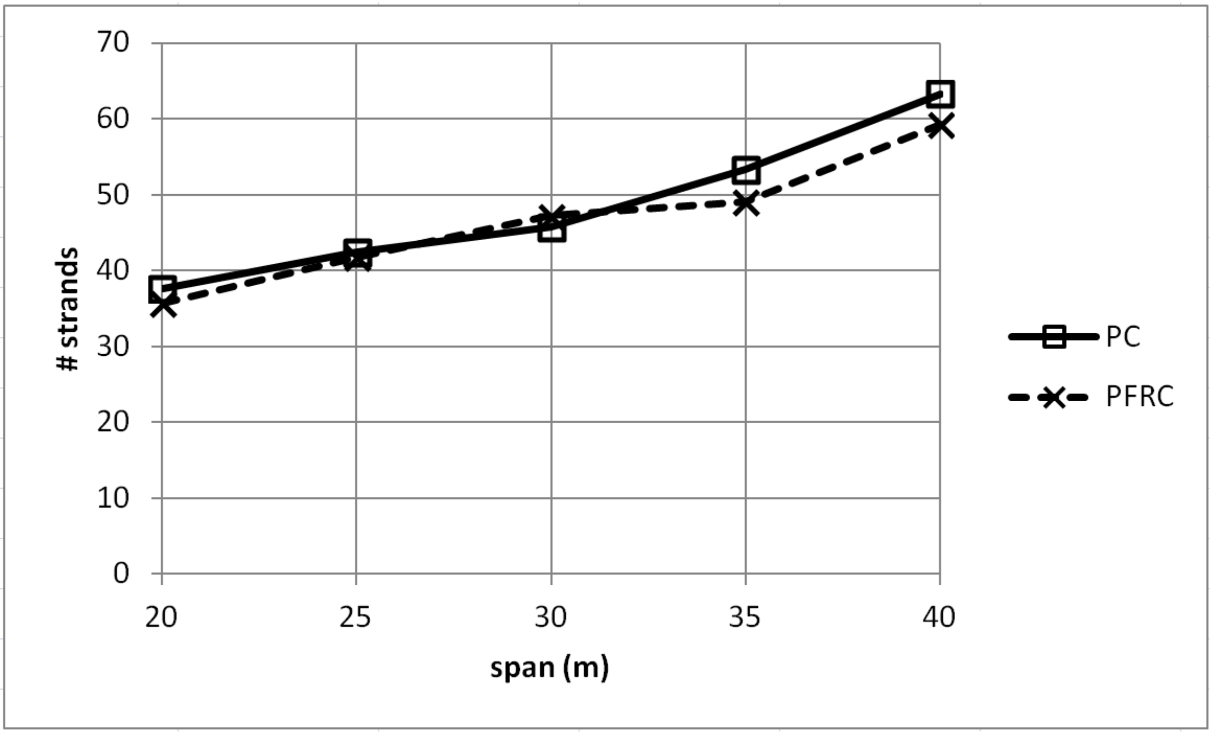


**Fig. 7.** Average number of strands in relation to the span lengths and use of fibers

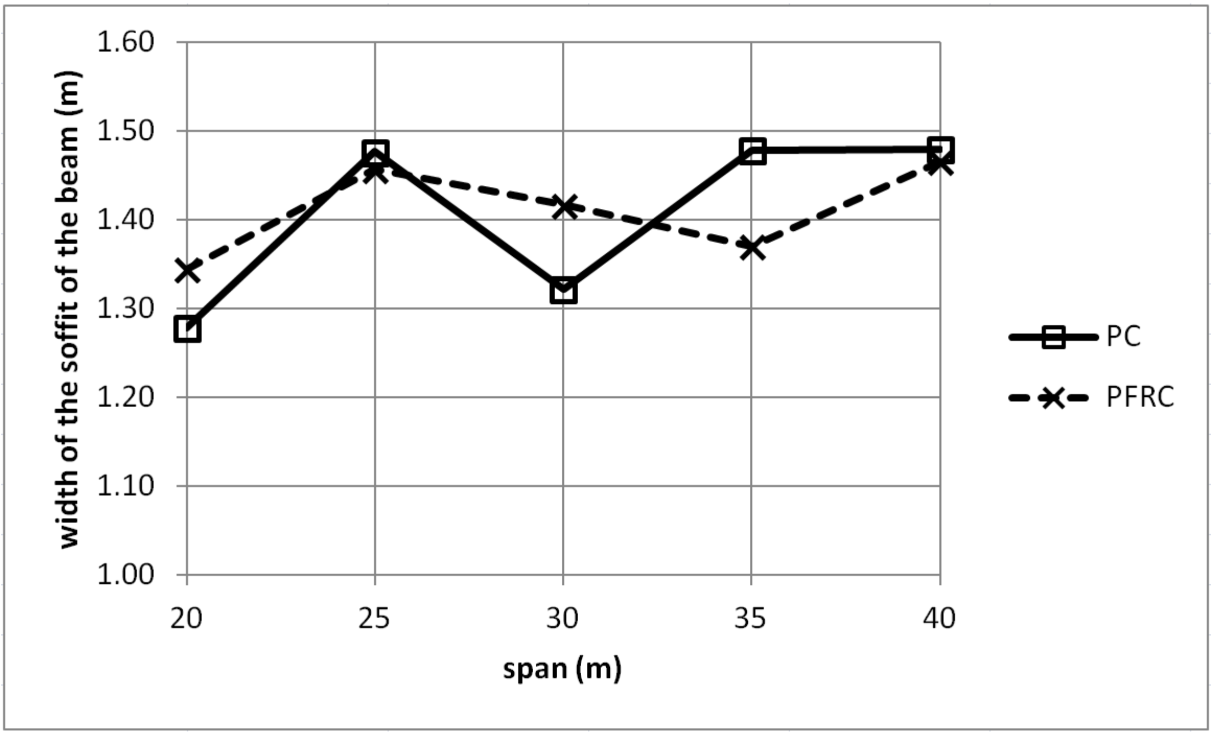


**Fig. 8.** Width of the soffit of the beam in relation to the span lengths and use of fibers

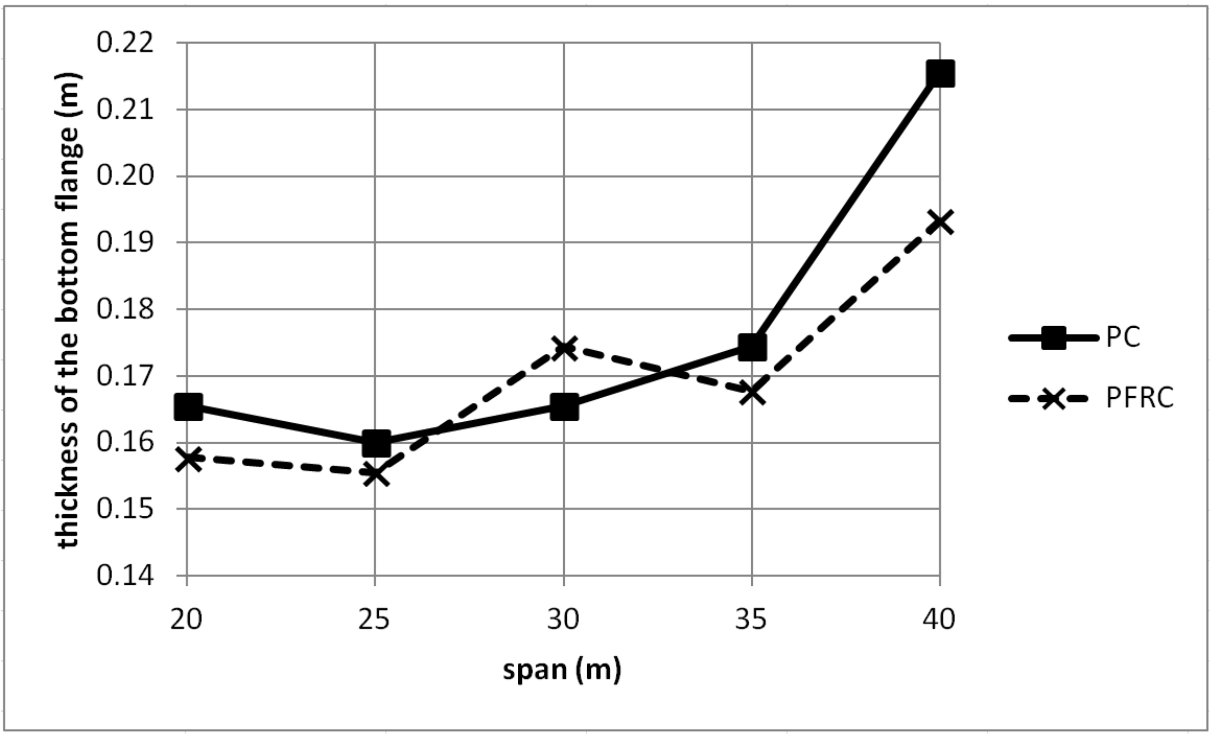


**Fig. 9.** Thickness of the bottom flange of the beam in relation to the span lengths and use of fibers

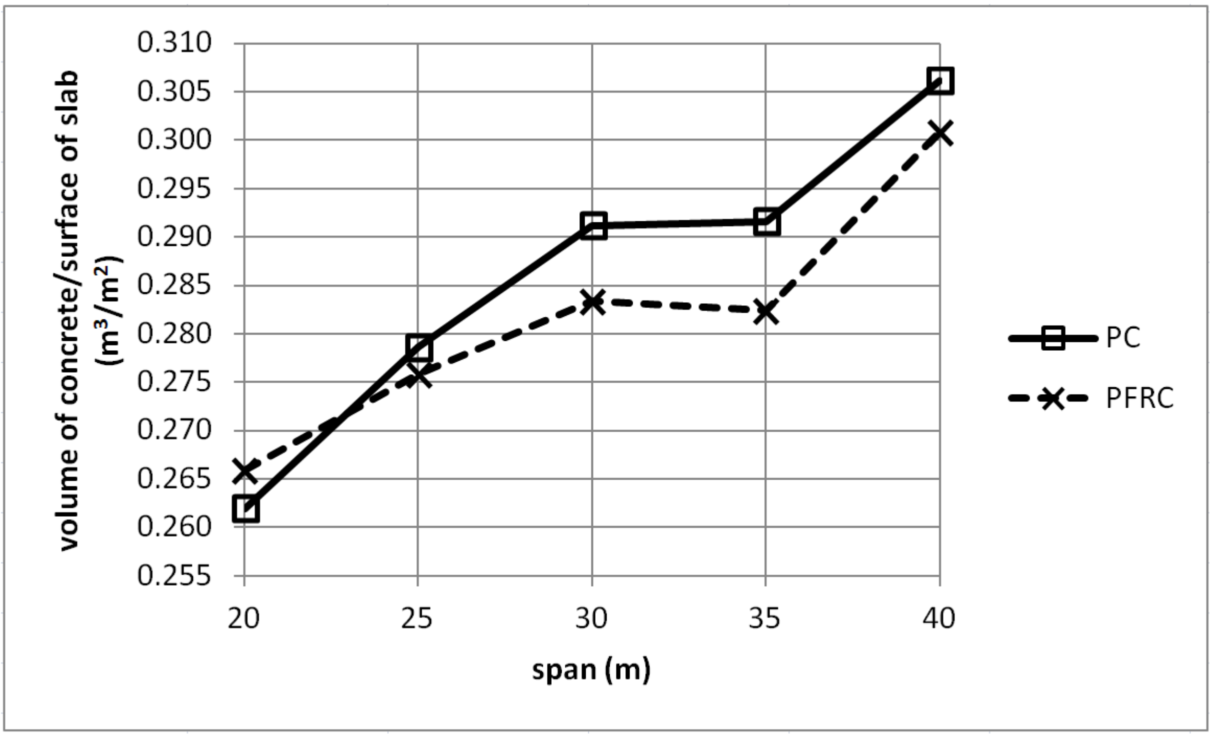


**Fig. 10.** Mean volume of concrete-to-surface of slab ratio in relation to the span lengths and use of fibers

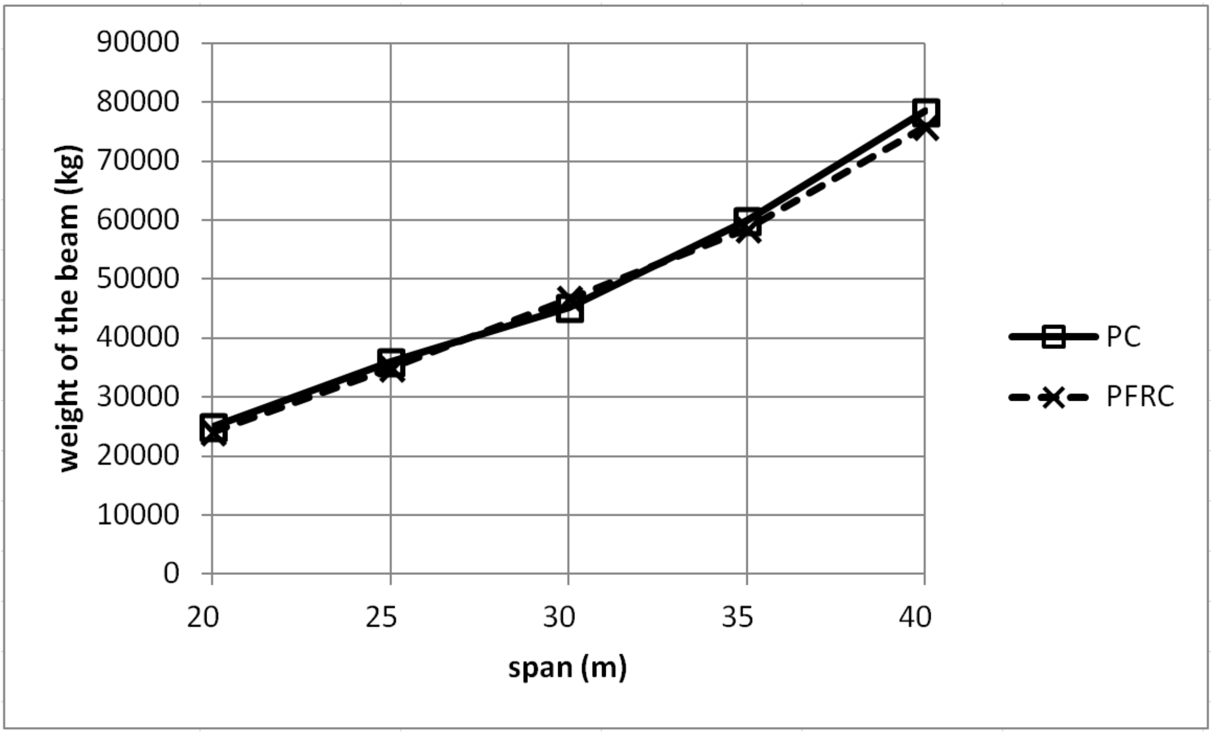


**Fig. 11.** Mean weight of the beam in relation to the span lengths and use of fibers

**Table 1.** Unit cost values.

| Input parameter | Unit | Value |
|---|---|---|
| Cost of beam steel (B-500-S) | US$/kg | 3.65 |
| Cost of slab steel (B-500-S) | US$/kg | 1.95 |
| Cost of active steel (Y1860-S7) | US$/kg | 4.71 |
| Cost of beam formwork | US$/m | 104.48 |
| Cost of slab formwork | US$/$m^2$ | 41.60 |
| Cost of slab concrete HA-25 | US$/$m^3$ | 91.00 |
| Cost of slab concrete HA-30 | US$/$m^3$ | 97.50 |
| Cost of slab concrete HA-35 | US$/$m^3$ | 104.00 |
| Cost of slab concrete HA-40 | US$/$m^3$ | 110.50 |
| Cost of beam concrete HP-35 | US$/$m^3$ | 170.05 |
| Cost of beam concrete HP-40 | US$/$m^3$ | 185.56 |
| Cost of beam concrete HP-45 | US$/$m^3$ | 197.73 |
| Cost of beam concrete HP-50 | US$/$m^3$ | 212.67 |
| Cost of beam steel fiber | US$/kg | 1.43 |

**Table 2.** Steel reinforcement, cost correction coefficients.

| Diameter (mm) | Beam | | Slab | |
|---|---|---|---|---|
| | Material | Labor | Material | Labor |
| D6 | 1.250 | 1.400 | 1.250 | 1.400 |
| D8 | 1.170 | 1.250 | 1.170 | 1.250 |
| D10 | 1.075 | 1.100 | 1.075 | 1.100 |
| D12 | 1.000 | 1.000 | 1.000 | 1.000 |
| D16 | 0.980 | 0.900 | 0.980 | 0.900 |
| D20 | 0.980 | 0.900 | 0.980 | 0.900 |
| D25 | - | - | 1.000 | 0.800 |
| D32 | - | - | 1.000 | 0.800 |

**Table 3.** Beam transport costs (distance up to 50 km/one way).

| Maximum beam weigh (kN) | Transport cost (US$) |
|---|---|
| 550 | 1356 |
| 660 | 1773 |
| 800 | 2295 |
| 1000 | 2538 |
| 2000 | 3929 |
| 4000 | 5320 |

**Table 4.** Beam placing costs.

| Maximum beam length (m) | Placing cost (US$) |
|---|---|
| 20 | 4034 |
| 25 | 4173 |
| 30 | 7094 |
| 35 | 7233 |
| 40 | 8624 |

**Table 5.** Input parameters for analysis.

| **Input parameter** | **Unit** | **Symbol** | **Value** |
|---|---|---|---|
| PC precast bridge width | m | $W$ | 12.00 |
| Inclination, top flange tablet | - | $n_{s3}$ | 3 |
| Top flange division | - | $s_3$ | 3 |
| Inclination, bottom flange tablet | - | $n_{i3}$ | 3 |
| Bottom flange division | - | $i_4$ | 4 |
| Web inclination | degree | $I_a$ | 80 |
| Beam slenderness | Span/$h_1$ | - | >17 |
| Bearing center to beam face distance | m | $E_{nt}$ | 0.47 |
| Concrete bridge barrier width | m | $a_{bar}$ | 2x0.50 |
| Thickness of wearing surface | m | $t_{ws}$ | 0.09 |
| Concrete bridge barrier loads | kN/m | $Q_m$ | 2x5.0 |
| Transport distance (one way) | km | $T_d$ | 50 |
| Active prestressing steel crops | % | | 25 |
| Passive reinforcing steel (B-500-S) | N/mm$^2$ | $f_{yk}$ | 500 |
| Active prestressing steel (Y1860-S7) | N/mm$^2$ | $f_{pk}$ | 1700 |
| Strand diameter | inches | $\Phi_s$ | 0.6 |
| Beam surface reinforcement | mm | $\Phi_r$ | 8 |
| Strand sheaths | Levels 2 and 3 | | |
| Stirrups, vertical slenderness | 200 (length/diameter) | | |

**Table 6.** MA-VDNS cost results from nine runs for 20-25-30-35-40 m spans.

| | PC | | | PFRC | | |
|---|---|---|---|---|---|---|
| Span (m) | Mean cost (US$) | Minimum cost (US$) | Deviation % | Mean cost (US$) | Minimum cost (US$) | Deviation % |
| 20 | 76,779 | 73,052 | 5.1 | 74,706 | 72,877 | 2.5 |
| 25 | 92,547 | 86,505 | 7.0 | 93,604 | 91,850 | 1.9 |
| 30 | 111,848 | 108,308 | 3.3 | 110,813 | 107,054 | 3.5 |
| 35 | 134,199 | 128,627 | 4.3 | 132,135 | 121,733 | 8.5 |
| 40 | 153,829 | 140,759 | 9.3 | 158,534 | 139,255 | 13.8 |

**Table 7.** MA-VDNS best solutions for 20-25-30-35-40 m spans.

| Span (m) | | $h_1$ (m) | $e_4$ (m) | $b_1$ (m) | $b_3$ (m) | $e_1$ (m) | $e_2$ (m) | $e_3$ (m) | $f_{c,beam}$ (MPa) | $f_{c,slab}$ (MPa) | $p_1$ (n) | $p_2$ (n) | $p_3$ (n) | $p_4$ (n) | $S_v$ (m) | $f_{r3k}$ (MPa) |
|---|---|---|---|---|---|---|---|---|---|---|---|---|---|---|---|---|
| 20 | a | 1.13 | 0.18 | 1.28 | 0.23 | 0.20 | 0.10 | 0.15 | 45 | 30 | 22 | 17 | 0 | 2 | 5.67 | - |
| | b | 1.07 | 0.18 | 1.45 | 0.25 | 0.15 | 0.11 | 0.10 | 40 | 35 | 26 | 8 | 0 | 4 | 5.65 | 4.0 |
| 25 | a | 1.35 | 0.19 | 1.26 | 0.23 | 0.15 | 0.10 | 0.15 | 35 | 25 | 22 | 22 | 0 | 2 | 5.39 | - |
| | b | 1.31 | 0.20 | 1.08 | 0.32 | 0.15 | 0.10 | 0.10 | 45 | 35 | 18 | 18 | 0 | 2 | 5.60 | 5.5 |
| 30 | a | 1.61 | 0.19 | 1.07 | 0.24 | 0.15 | 0.10 | 0.17 | 35 | 35 | 18 | 18 | 0 | 4 | 5.67 | - |
| | b | 1.65 | 0.18 | 1.22 | 0.30 | 0.19 | 0.10 | 0.15 | 35 | 30 | 21 | 21 | 0 | 2 | 5.73 | 6.0 |
| 35 | a | 1.83 | 0.17 | 1.33 | 0.23 | 0.16 | 0.10 | 0.16 | 45 | 30 | 23 | 23 | 0 | 2 | 5.46 | - |
| | b | 1.78 | 0.17 | 1.35 | 0.23 | 0.15 | 0.10 | 0.15 | 40 | 30 | 24 | 24 | 0 | 2 | 5.61 | 5.0 |
| 40 | a | 2.07 | 0.18 | 1.29 | 0.23 | 0.18 | 0.10 | 0.15 | 35 | 40 | 22 | 22 | 0 | 2 | 5.64 | - |
| | b | 2.11 | 0.17 | 1.25 | 0.25 | 0.15 | 0.10 | 0.11 | 35 | 25 | 22 | 22 | 0 | 2 | 5.25 | 3.0 |

(a) PC
(b) PFRC

**Table 8.** MA-VDNS basic measurements for 20-25-30-35-40 m spans.

| Span (m) | | Beam reinforcement (kg) | Slab reinforcement (kg) | Total reinforcement (kg/m$^2$) | Beam concrete (m$^3$/m$^2$) | Slab concrete (m$^3$/m$^2$) |
|---|---|---|---|---|---|---|
| 20 | a | 2,794 | 8,137 | 43.38 | 0.079 | 0.183 |
| | b | 1,666 | 8,938 | 42.08 | 0.076 | 0.189 |
| 25 | a | 3,645 | 8,740 | 39.69 | 0.092 | 0.186 |
| | b | 2,107 | 11,830 | 44.67 | 0.090 | 0.186 |
| 30 | a | 5,399 | 10,089 | 41.63 | 0.097 | 0.194 |
| | b | 3,673 | 11,756 | 41.47 | 0.100 | 0.183 |
| 35 | a | 6,895 | 11,562 | 42.73 | 0.111 | 0.181 |
| | b | 4,377 | 15,318 | 45.59 | 0.108 | 0.174 |
| 40 | a | 7,968 | 10,343 | 37.22 | 0.128 | 0.179 |
| | b | 5,778 | 17,598 | 47.51 | 0.123 | 0.178 |

(a) PC

(b) PFRC